Channel length specific broadspectral photosensitivity of robust chemically grown CdS photodetector

Alka Sharma, Mandeep Kaur, Biplab Bhattacharyya, Stalin Karuppiah, Surinder P. Singh, T. D. Senguttuvan, and Sudhir Husale

Articles you may be interested in

CdS quantum dots grown by in situ chemical bath deposition for quantum dot-sensitized solar cells
J. Appl. Phys. **110**, 044313 (2011); 10.1063/1.3624944

Temperature Dependent Photosensitivity of Cu Doped CdS Thin Film
AIP Conf. Proc. **1349**, 267 (2011); 10.1063/1.3605837

Conversion of chemically deposited photosensitive CdS thin films to n-type by air annealing and ion exchange reaction
J. Appl. Phys. **75**, 1557 (1994); 10.1063/1.356391

Structural characterization of CdS epilayers by channeling Rutherford backscattering spectrometry
J. Appl. Phys. **70**, 2041 (1991); 10.1063/1.349463

Crystallography of CdTe layers on CdS grown by chemical vapor transport
J. Appl. Phys. **50**, 869 (1979); 10.1063/1.326002

Channel length specific broadspectral photosensitivity of robust chemically grown CdS photodetector

Alka Sharma,[1,2] Mandeep Kaur,[2] Biplab Bhattacharyya,[1,2] Stalin Karuppiah,[2] Surinder P. Singh,[1,2] T. D. Senguttuvan,[1,2] and Sudhir Husale[1,2,a]

[1]*Academy of Scientific and Innovative Research (AcSIR), National Physical Laboratory, Council of Scientific and Industrial Research, Dr. K. S Krishnan Marg, New Delhi-110012, India*
[2]*National Physical Laboratory, Council of Scientific and Industrial Research, Dr. K. S Krishnan Marg, New Delhi-110012, India*

CdS grown by chemical bath deposition (CBD) technique is very simple, robust, economical method and has potential large scale applications in solar cells, photovoltaic, photodetectors, sensors and optoelectronic devices. Here we report channel lengths (CLs) specific broadspectral photoresponse properties of commonly grown robust CdS films by CBD. The broadspectral dependent current flow has been observed in all CLs and the rise and decay times have been measured in milliseconds for visible wavelengths (400-700nm). The rise time curves showed linear dependency when measured for CLs 300, 500 and 700nm and non-linearity was observed for CLs 7μm, 45μm and 350μm. We have noticed that decrease in channel lengths down to nanometers (300 nm) increases the response time. Three steps decay time has been noticed for all CLs. The shorter channels (nm) showed two trends in decay time, small increase for wavelengths < 550nm and significant increase for wavelengths > 550nm. Finally, CLs specific broadspectral photosensitivity has been investigated which indicates the device geometry and fabrication method play an important role for defining the CdS based photodetectors or simulating the characteristics of a photodetector. © *2015 Author(s). All article content, except where otherwise noted, is licensed under a Creative Commons Attribution 3.0 Unported License.* [http://dx.doi.org/10.1063/1.4918270]

INTRODUCTION

CdS (cadmium sulfide), group II-VI semiconductor, is very fascinating and potential candidate for making optoelectronic devices due to direct band gap, excellent photoconductivity, good chemical, thermal stability and relative low work function. Many promising studies have been revived already[1] and have been reported its applications in photodetectors, light emitting diodes (LED), field-emitters, transistors, sensors and solar cells etc. Recently, nanostructures of CdS have attracted lots of attentions due to excellent properties such as photoresponse, high sensitivity, high detectivity[2] photocatalytic activity,[3] stability, fast speed etc.,[4] But synthesis of nanoscale structures need high temp growths and device fabrication requires sophisticated lithography processes. However, solution based techniques are more economical and efficient for large scale production of nano film based photodetectors.[5]

Chemical bath deposition (CBD) [6–17] is the most commonly used technique to make CdS thin films and have been studied heavily for their photodynamics, electro-optical studies and also known low cost material for photodetector applications. One of the big advantages of CBD method is that film can be made over a large area (mm^2). But quality of films depends on many factors like substrate, orientation and agitation, thickness,[18] grain size, deposition technique,[19,20] bath

---

[a]Email: husalesc@nplindia.org

temperature,[21] optical absorption, crystalline structure, Cd and S defects,[22] solution pH,[23] annealing[24] etc. It is difficult to maintain all these parameters when large scale production or industry level technological applications are considered. Importance is to have simple method for making a robust film, cost effective, highly reproducible, showing mechanism with easily achievable sensitivity. Further, when simple and robust thin films prepared and scaling down of device's physical dimensions are considered, photodetection technology applications may demand electro-optical studies on short or long channel lengths, their broadspectral photoresponse need to predict accurately, particularly rise or decay time. To the best of our knowledge, CBD grown CdS films have not been characterized for their broader spectral response specific to the effects of channel lengths (CLs) on rise and decay time.

Here we focused on robust films of CdS made by CBD technique and it is evaluated for CLs from few hundreds nm to μm scale. Films by CBD technique usually have impurities; large grain sizes hence could be ample trapped states. The defects formed in the films may not be uniform, but could directly affect the electrical properties depending on the length of the cannel formed and thus performance of the detector. Photodetector having broader spectral response effectively can convert optical signal into an electrical signal hence it is important to investigate the broad spectral sensitivity of the photodetector in particular to rise and decay time specific to the CLs. The influence of CLs on broadspectral photoreponse (rise and decay time) is reported here. Results presented here indicate that rise and decay time may be fitted with linear relation for device geometry in nm but photoresponse show non-linearity when devices made in μm range. From the rise time, nanochannels show fast kinetics for broad spectral response.

RESULTS AND DISCUSSIONS

CdS thin films on SiO$_2$/Si and glass substrates were prepared from a chemical bath containing 0.004M cadmium chloride (CdCl$_2$), 0.04M ammonium chloride (NH$_4$Cl), 0.004M thiourea (H$_2$NCSNH$_2$) and 5% ammonium hydroxide (NH$_4$OH). Prior to deposition of CdS thin films, all substrates were properly cleaned with acetone, isopropanol, methanol and distilled water respectively. The cadmium chloride and ammonium chloride were dissolved in one beaker whereas thiourea was dissolved in another beaker with the help of magnetic beads. The temperature of the bath was maintained at 65-70°C. Thiourea was added slowly in the above solution where substrates were already placed in the beaker and stirring rate was maintained. Growth of the film was continued until the colour of the solution was changed to pale yellow and it took ∼ 20 min to complete the reaction time. After deposition, substrates were mild ultrasonicated for few sec in water bath to remove the loosely attached particles. Deposited CdS films were characterized by FESEM (field emission scanning electron microscope), XRD (x-ray diffraction) and UV-absorption spectroscopy. For the electrical measurements, gold electrodes (Ti = 10nm, Au = 90nm) were deposited on CdS thin film by sputtering method. The room temperature electrical measurements were carried out in the probe station (Cascade Microtech, low noise EMI shielding) with the help of source meter 2634B and 2400 (Keithley Instruments Inc.). Halogen lamp and filters of specific wavelengths (400, 480, 550, 600, 660, 700nm) were used to illuminate the devices in perpendicular direction. Optical power was measured over an area 1 cm^2. Different CLs (distance between source electrode and drain electrode) (300 nm, 500 nm, 700 nm, 7 μm, 15 μm, 45 μm and 350 μm) were used to probe the broad spectral photoresponse of CdS films.

Fig. 1(a) represents the FESEM image of as deposited CdS film on SiO$_2$/Si substrate which show granular morphology having grain sizes of ∼ 50 to 200 nm. Fig. 1(b) shows the X-ray diffraction pattern of CdS thin film reveals that film is polycrystalline in nature. This diffraction pattern indicates that there are two peaks, one which is intense at 26.81° which correspond to (111)plane and other which have relatively less intensity is at 44.27 which correspond to (220)plane. These peaks were matched with JCPDS card no.(89-0019). Figure 1(c) shows the absorption spectra of CdS thin film recorded for the wavelength range 400nm to 700nm. The inset shows the absorption coefficient and band gap was found to be ∼ 2.42 eV.

Fig. 1(d) shows the optical micrograph of the device, gold pads were deposited on CdS films for the electrical characterization and it was made by a simple shadow mask technique. Fig. 1(e)
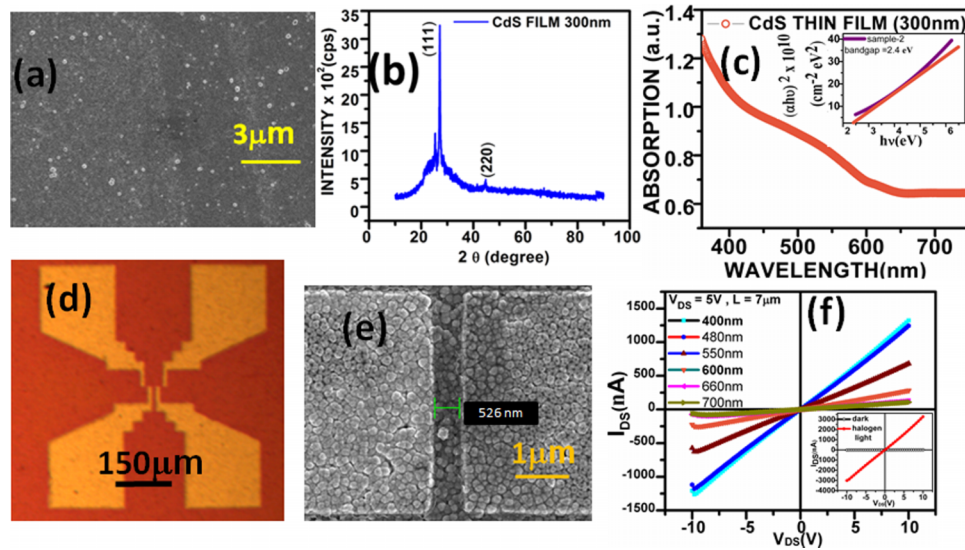
FIG. 1. Fig. 1(a) shows the FESEM image of the CdS film, (b) is the X-ray diffraction data and (c) is the UV absorption spectra of the film. Fig. 1(d) is the optical image of the device prepared by shadow masking and 1(e) is the FESEM image of the device fabricated by ebeam lithography. Fig. 1(f) represents the electrical response of the device under light illumination of different wavelengths.

shows the FESEM image of the device geometry made by ebeam lithography technique to study the broad spectral photoresponse. Figure 1(f) displays the current-voltage (I–V) curves of CdS films under the illumination of different wavelengths of light. Drastic change in electrical conductivity has been observed when wavelength was switched from 400nm to 700nm. IV curves indicate that photoconductivity of CdS film is spectral dependent and it is highly resistive in the dark or near IR region. Further, the films are photosensitive, response well to the incident light and electrical properties can be tuned with illumination of specific light.

Figs. 2(a) & 2(b) display the time-dependent photoresponse of CdS _ CBD films at constant bias voltage 5V for channel length 15 μm and 300 nm respectively. Photocurrent was observed rising rapidly when the light was switched ON and reaching to a saturation value. The rapid decay was also observed when the light was switched off which is as shown in the figs. (a) & (b).

The broadspectral photocurrent rise and decay was observed for both CLs when illuminated under wavelengths of 400, 480, 550, 600, 660 and 700nm. The increase in photocurrent at higher wavelengths (>550nm) as shown in Figs. 2(a)&2(b) which could be due to the presence of defects and might help carriers to move from valance band to conduction band. Thus robust films are with defects and may generate delocalized charge carriers at higher wavelengths. Figs. 2(c) & 2(d) represent the normalized data to get the rise and decay time. Data for all the rise time was fitted with the equation $I = Io\left(1 - e^{-\frac{t}{\Gamma}}\right)$ and for decay time it was fitted with the equation $I = Io\, e^{-t/\tau}$ where I is the photocurrent, Γ is the rise time and τ is the decay time. All the values of rise times for various CLs have been shown in Table 1 (in Ref. 25). On an average, we have observed fastest response (rise, 60 ms) time for shorter channel length (300nm) and slightly more rise time ~100 ms was observed for the CLs in μm scale. Note that, all the devices measured here showed very good stability, measurements on some devices were also performed in days or week's interval time. Figs. 2(e) and 2(f) represent the decay data of respective CLs. Decay in all CLs, was observed and characterize by three step process, decay1, 2 and 3 where step1 is fast process in ms, step2 and 3 are slow processes usually in few secs time scale. Solid curve lines show the fits by using above exponential decay equation and fitted values of all τ have been shown in Table 1 (in Ref. 25). The data shown in the table1 is important for defining the sensitivity of CBD grown CdS films and the device geometry tuning.
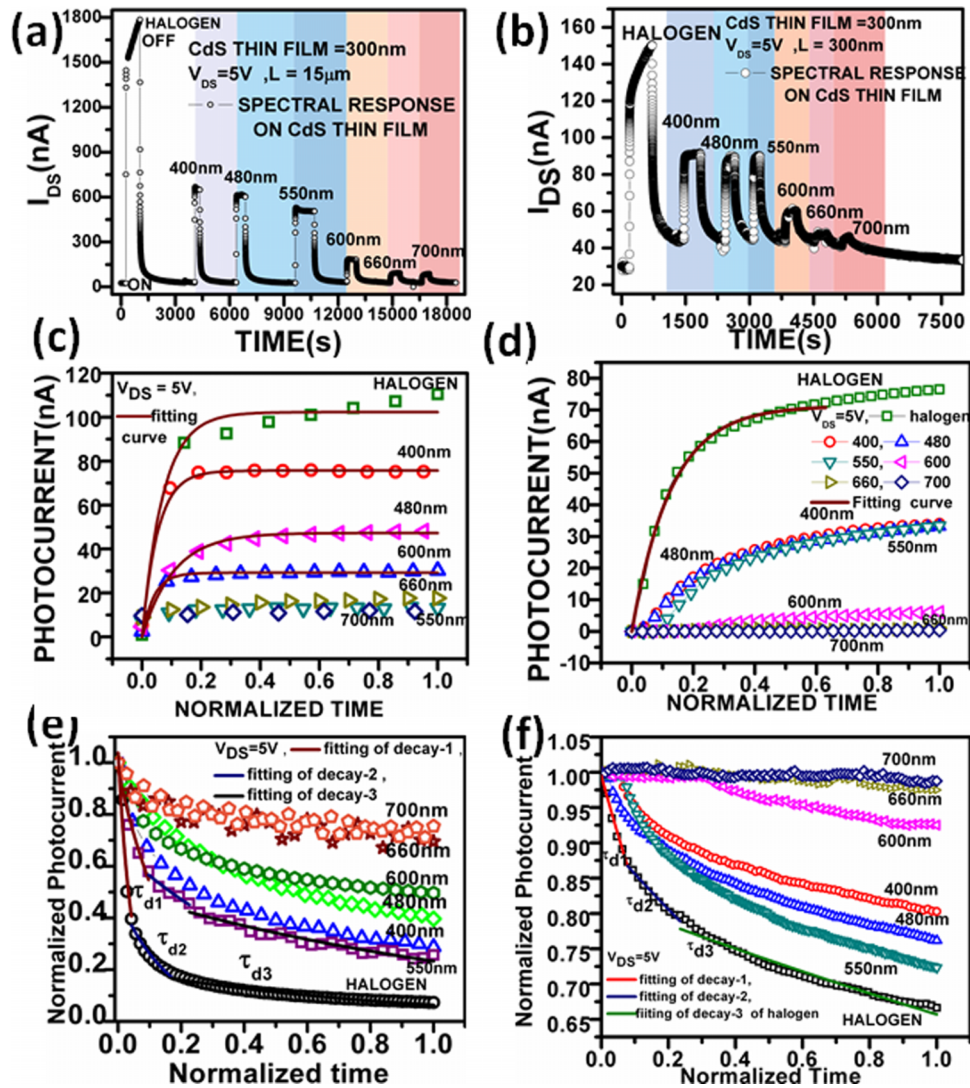
FIG. 2. (a&b) show the time dependent photocurrent measurements done on CdS films for CLs 15 μm and 300 nm. Figs. (c)&(d) illustrate the normalized photocurrent curves fitted (solid lines) for rise time when light was ON and figs. (e)&(f) show the normalized decay curves fitted for 3 decay times (solid lines) when light was OFF.

Fig. 3(a) shows the CLs dependent broad photospectral rise time. For each CLs, measurements were done on minimum three devices. Note that many devices were fabricated on single CdS deposited SiO$_2$/Si substrate. Solid lines are the linear fits and values of the slopes are given in the table 2A (in Ref. 25). The rise time increases linearly and small incremental change has been observed for all the devices. It clearly indicates that film sensitivity can be tuned if optical signal characterized at different CLs. Scaling down CLs from 700nm to 300nm, ∼ 2 times improvement has been observed in photocurrent rise time and it was consistent for all the wavelengths with small variations. The rise time for channel length 350 μm was observed ∼ 300 ms. This suggests the enhancement factor of 4 can be obtained if device geometry was reduced to 3 order. The increase in rise time is simply could be due to the channel length increase which increase time of carriers to move in the channel, and possibility of more density grain boundaries that could obstruct the charge carries to move from valance band to conduction band. Note that increase in wavelength means decrease in energy to shift charge carriers from valence band to conduction band and decrease in rise time could be observed. Additionally we have performed the time dependent photocurrent measurements with on off cycles of a fixed wavelength and observed no time dependent significant change on the response
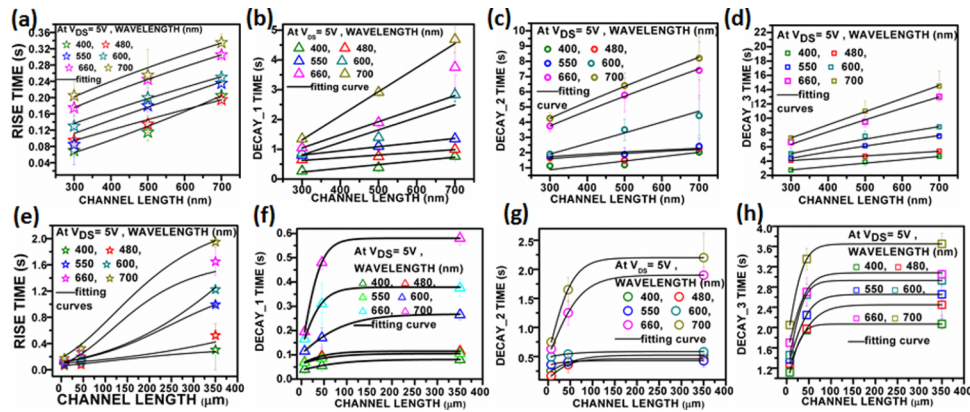
FIG. 3. Figs. 3(a) and 3(b)-3(d) show the rise and decay times for the short channels (nm) respectively. Figs. 3(e) and 3(f)-3(h) show the rise and decay times for the long channels (um) respectively.

or decay time which is shown in supplementary material (in Ref. 25). Previously rise and decay time of CdS nanostructures have been observed in ms as well as μs timescale. Jie *et al.* reported width dependent rise and decay time, (170 and 365 μs) for nanoribbon width of 10.4 um, but it was in millisecond for ribbon width 33 μm (1.4 ms, two decays 3.5 ms and 55.6 ms)[26] Other reports of CdS nanoribbons showed rise and decay time (551 μs and 1.093 ms),[27] (1 sec and 3sec)[28] and 31 ms decay time for CdS belt synthesized by the vapour phase transportation method.[29] The rise and decay time for CdS nanowire (15 ms)[30] and the aligned networks (0.8, 240 ms) have been also reported earlier.[10] It is important to note that, no distinct photoresponse was observed for the pure CdS nanobelt at higher wavelengths (> 532 nm)[26] but distinct photorespose was noticed for energy smaller than the bad gap when the CdS nanowire was doped with tin.[31] We cannot compare rise and decay with nanostructures or crystalline quality materials but CLs investigations may be studied further or improved for better quality films.

For deacy1 (Fig. 3(b)), two trends were observed, small increase in decay time for wavelengths < 550 nm but there was significant increase in decay1 for wavelengths > 550nm as CLs was increased. Decay2 and 3 also showed trend similar to decay1 (Figs. 3(c) and 3(d)). For the CLs in μm range, slight increase in response time (Fig. 3(e)) was observed for < 480nm but it was significant for wavelengths > 480nm. Decay1 and 2 (Figs. (f)&(g)) showed nonlinear trend, table2B (in Ref. 25). Decay 3 (Fig. 3(h)) showed significant increase in decay time for all the wavelengths. Here we can say that for particular wavelengths (energy close to the band gap of CdS) decay1&2 defects /grain boundaries are not affecting notably but do for higher wavelengths. For polycrystalline CdS films, it has been reported that if energy of light illumination is < than the band gap of the material (subband-gap) then photocurrent moves through grain boundaries only but it flows through grains as well as grain boundaries for energy > illumination of light.[6] Possibility that grain boundaries holds most of the charge carriers or delays the recombination of hole-electron which gives longer decays. However for short channels more decay time has been observed which may be due to the trapping of charge carriers at the grain boundaries and not easily available for conduction. Note that, nanogaps were fabricated with ebeam lithography process which could add more defects or openings in the film (Fig. 1(e)). This indicates that hole–electron recombination is wavelength and grain boundary specific and needs to investigate more specific to the samples fabricated by various lithography processes.

CONCLUSION

CdS films prepared by CBD technique were characterized for their CLs specific broadspectral photoresponse. Simple shadow mask was used to make devices of CLs down to few microns which showed good ohmic contacts and noticeable photoresponse was observed for the energy less than the band gap. The electro-optical characterization of the thin film at micro and nanoscale gives

new insights to rise and decay process and supports that defects in the film obstruct decay time. The shorter channels (nm) confirm that rise time can be improved (2X); hence the photosensitivity may affect due to the device geometry of the channel length. Photocurrent decay was observed wavelength dependence and it showed linear dependency for shorter channels but nonlinearity for longer channels. Comparatively slow rise or decay indicates defects and grain boundaries present in the film. It has been suggested that the trapping centres, such as the defects introduced by the ebeam lithograpy process, may increase the decay speed. Moreover, photo detector applications rely on the broad spectral photocurrent generation, rise and decay time largely depends on nano or microscale area. Further, CdS films if combined with graphene may enhance the photoresponse properties for future applications in fast electronic devices. The results presented here could be useful to define or simulate photoresponse properties of a simple, cost effective, large scale CBD grown CdS photodetctor.

[1] T. Zhai, X. Fang, L. Li, Y. Bando, and D. Golberg, Nanoscale **2**(2), 168-187 (2010).
[2] J. He, J. Chen, Y. Yu, L. Zhang, G. Zhang, S. Jiang, W. Liu, H. Song, and J. Tang, J Mater Sci: Mater Electron **25**(3), 1499-1504 (2014).
[3] S. Han, L. Hu, N. Gao, A. A. Al-Ghamdi, and X. Fang, Advanced Functional Materials **24**(24), 3725-3733 (2014).
[4] K. Deng and L. Li, Advanced Materials **26**(17), 2619-2635 (2014).
[5] X. Wang, W. Tian, M. Liao, Y. Bando, and D. Golberg, Chemical Society Reviews **43**(5), 1400-1422 (2014).
[6] D. Azulay, O. Millo, S. Silbert, I. Balberg, and N. Naghavi, Applied Physics Letters **86**(21), 212102 (2005).
[7] C. Voss, S. Subramanian, and C.-H. Chang, Journal of Applied Physics **96**(10), 5819-5823 (2004).
[8] O. Demelo, L. Hernandez, O. Zelayaangel, R. Lozadamorales, M. Becerril, and E. Vasco, Applied Physics Letters **65**(10), 1278-1280 (1994).
[9] H. Metin and R. Esen, Semiconductor Science and Technology **18**(7), 647-654 (2003).
[10] K. Heo, H. Lee, Y. Park, J. Park, H.-J. Lim, D. Yoon, C. Lee, M. Kim, H. Cheong, J. Park, J. Jian, and S. Hong, Journal of Materials Chemistry **22**(5), 2173-2179 (2012).
[11] H. Khallaf, I. O. Oladeji, G. Chai, and L. Chow, Thin Solid Films **516**(21), 7306-7312 (2008).
[12] M. A. Islam, M. S. Hossain, M. M. Aliyu, P. Chelvanathan, Q. Huda, M. R. Karim, K. Sopian, and N. Amin, Energy Procedia **33**(0), 203-213 (2013).
[13] H. Moualkia, S. Hariech, M. S. Aida, N. Attaf, and E. L. Laifa, Journal of Physics D-Applied Physics **42**(13) (2009).
[14] A. Asikoglu and M. H. Yukselici, Semiconductor Science and Technology **26**(5) (2011).
[15] J. Kokaj and A. E. Rakhshani, Journal of Physics D-Applied Physics **37**(14), 1970-1975 (2004).
[16] H. Zhang, X. Y. Ma, J. Xu, J. J. Niu, J. Sha, and D. R. Yang, Journal of Crystal Growth **246**(1-2), 108-112 (2002).
[17] H. Zhang, X. Y. Ma, J. Xu, and D. R. Yang, Journal of Crystal Growth **263**(1-4), 372-376 (2004).
[18] J. P. Enriquez and X. Mathew, Solar Energy Materials and Solar Cells **76**(3), 313-322 (2003).
[19] S. Rubio, J. L. Plaza, and E. Dieguez, Journal of Crystal Growth **401**, 550-553 (2014).
[20] X. Li, W. Li, and X. Dong, Japanese Journal of Applied Physics Part 1-Regular Papers Brief Communications & Review Papers **45**(12), 9108-9110 (2006).
[21] F. Y. Liu, Y. Q. Lai, J. Liu, B. Wang, S. S. Kuang, Z. A. Zhang, J. Li, and Y. X. Liu, Journal of Alloys and Compounds **493**(1-2), 305-308 (2010).
[22] K. S. Ramaiah, R. D. Pilkington, A. E. Hill, R. D. Tomlinson, and A. K. Bhatnagar, Materials Chemistry and Physics **68**(1-3), 22-30 (2001).
[23] S. Prabahar and M. Dhanam, Journal of Crystal Growth **285**(1-2), 41-48 (2005).
[24] D. Quinonez-Urias, A. Vera-Marquina, D. Berman-Mendoza, A. L. Leal-Cruz, L. A. Garcia-Delgado, I. E. Zaldivar-Huerta, A. Garcia-Juarez, A. G. Rojas-Hernandez, and R. Gomez-Fuentes, Optical Materials Express **4**(11), 2280-2289 (2014).
[25] See supplementary material at http://dx.doi.org/10.1063/1.4918270 for channel length specific rise and decay times (Table 1), linear fit (Table 2A) and nonlinear fit parameters (Table 2B).
[26] J. S. Jie, W. J. Zhang, Y. Jiang, X. M. Meng, Y. Q. Li, and S. T. Lee, Nano Letters **6**(9), 1887-1892 (2006).
[27] L. Yingkai, Z. Xiangping, H. Dedong, and W. Hui, J Mater Sci **41**(19), 6492-6496 (2006).
[28] T. Gao, Q. H. Li, and T. H. Wang, Applied Physics Letters **86**(17) (2005).
[29] L. Li, S. Yang, F. Han, L. Wang, X. Zhang, Z. Jiang, and A. Pan, Sensors **14**(4), 7332-7341 (2014).
[30] Q. Li and R. M. Penner, Nano Letters **5**(9), 1720-1725 (2005).
[31] W. Zhou, Y. Peng, Y. Yin, Y. Zhou, Y. Zhang, and D. Tang, AIP Advances **4**(12), 123005 (2014).